# POLSAR IMAGE SPECKLE REDUCTION BASED ON SPARSE REPRESENTATION AND STRUCTURE CHARACTERISTICS

*Ping Han* [1] *Xiaohong Yu* [2] *Xiaoguang Lu* [1] *Hai Li* [1]

1. Tianjin Key Lab for Advanced Signal Processing, Civil Aviation University of China, Tianjin 300300, China
2. CETC Infrared Engineering and Technology Co., Ltd, Beijing 100015, China
Email: hanpingcauc@163.com

## ABSTRACT

This paper presents a novel speckle reduction algorithm based on sparse representation and structure characteristics of PolSAR image. First, each pixel in original image is classified into bright point or line targets, dark point or line targets and others to form a classification map. Second, sparse decomposition and reconstruction is performed on PolSAR image by OMP and K-SVD methods to filter speckle. Finally, the blurred point and line targets in filtered image are enhanced with the classification map. Experimental results with the data of Hayward area from AIRSAR system show that the proposed method is effective both on speckle reduction and scattering characteristics preservation.

***Keywords*—**PolSAR image; speckle reduction; sparse representation; structure classification map; polarimetric characteristics .

## 1. INTRODUCTION

In recent years, sparse decomposition has been successfully applied in image processing, such as image denoising, segmentation and target classification, etc. [1-5]. In 2008, sparse decomposition was used in SAR image speckle reduction [6], which shows it can suppress the speckle noise effectively and provides us a new speckle filtering idea. But during the sparse denoising process, some point or line targets with lower scattering power and some isolated point targets in original image can be suppressed easily as noise. Meanwhile, target edges in image also become blurred easily.

To overcome the above problems in literature [6], a novel speckle reduction algorithm is proposed in this paper. First, each pixel is classified into one of the following three types of targets, which are bright point or line targets, dark point or line targets and other targets, to form a classification map[7]; Then sparse decomposition and reconstruction are applied on PolSAR image to filter speckle. Last, some blurred point and line targets induced by filtering are enhanced with classification map. Experimental results show that the algorithm can not only suppress speckle noise effectively, but also keep the point and line targets with lower scattering power clear. Meanwhile, the image polarimetric feature and texture information are also well protected.

## 2. IMAGE DENOISING BASED ON SPARSE DECOMPOSITION

### 2.1. Image Sparse Decomposition and Reconstruction

Suppose $f$ is a noisy image, with size $M_1 \times M_2$ . Decomposing it on a over-complete dictionary D, the sparse representation of $f$ can be obtained normally . $f$ can be expressed as [8]:

$$f = \sum_{k=0}^{\infty} < R^k f, g_{\gamma_k} > g_{\gamma_k} \tag{1}$$

Where $D = \{g_\gamma\}$, subject to $\|g_\gamma\| = 1$ , $\gamma(\gamma = 1, 2, \ldots \Gamma)$ . $R^k f$ is the residual vector after projecting $f$ or $R^{k-1} f$ in the direction of $g_{\gamma_{k-1}}$ .Actually, according to the decay characteristic of $\|R^n f\|$ , using a small number of atoms can represent the major components of image:

$$f \approx \sum_{k=0}^{n-1} < R^k f, g_{\gamma_k} > g_{\gamma_k} \tag{2}$$

$n << M_1 \times M_2$ , equation (2) and the condition $n << M_1 \times M_2$ embodies the idea of image sparse representation.

For any image $f$ , we can describe it as follows:

$$f = f_s + f_n \tag{3}$$

Where:

$$f_s = \sum_{k=0}^{n-1} \left\langle R^k f, g_{\gamma_k} \right\rangle g_{\gamma_k} \tag{4}$$

$$f_n = \sum_{k=n}^{\infty} \left\langle R^k f, g_{\gamma_k} \right\rangle g_{\gamma_k} \tag{5}$$

$f_s$ is the image sparse component; $f_n = f - f_s$ is the residual component (also can be considered as noise).

Image reconstruction is described as: the sparse component of image $f$ are obtained by sparse decomposition on a dictionary D. By training D, we can get the most sparse components $\hat{\alpha}$ . Then a noiseless image is reconstructed with $\hat{\alpha}$ and a trained $\hat{D}$ . There are several methods to calculate $\hat{\alpha}$ , such as Matching Pursuit (MP), Orthogonal Matching Pursuit (OMP) and Basic Pursuit (BP) method etc [9-10].

If image noise is additive white Gaussian, MAP estimation value of the reconstructed image by sparse decomposition is proposed [11]:

$$\{\hat{\alpha}_{ij}, \hat{D}, \ldots \quad {}_{D,\alpha_{ij},x} \quad \ldots \sum_{i,j} \ldots \sum_{i,j} \ldots \tag{6}$$

Where, $\lambda$ is Lagrange multiplier, $\alpha_{i,j}$ is an element in the sparse coefficient matrix $\alpha$ , D is the dictionary; $\hat{D}$ and $\hat{\alpha}$ are the optimal solution of D and $\alpha$ . $\tilde{x}$ is the reconstructed image. On the right of equation (6), the first term represents the error between $f$ and $\tilde{x}$ ; the second one is sparse prior conditions ; the third one expresses the prior conditions for the consistency of image decomposition, in order to ensure the first term minimum. $R_{ij}\tilde{x}$ indicates a image sub-block around pixel $(i, j)$ , its size is normally $8 \times 8$ . Hence the filtering equation can be obtained:

$$\tilde{x} \quad \sum_{i,j} R_{ij}^T R_{ij})^{-1}(\lambda f + \sum_{i,j} R_{ij}^T \hat{D}\hat{\alpha}_{ij}) \tag{7}$$

Where $I$ is the unit matrix.

### 2.2. Sparse Denoising

Speckles in SAR image are multiplicative noise. For a observed SAR power image $f_I$ , it can be described as a product of two independent random variables:

$$f_I = SX \tag{8}$$

Where $X$ and $S$ are radar reflectivity and speckle noise respectively, By doing logarithmic transformation on SAR power image , the speckle noise becomes additive:

$$\tilde{\ } \quad = \tilde{\ } \quad \tilde{\ } \tag{9}$$

If we apply equation (7) in equation (9) directly, it will cause the following two problems :

1) Logarithmic transformation for SAR image brings certain deviation;

2) It can induce a potential bias if $\lambda > 0$ ( $E[\tilde{\ } \quad {}_{\lambda+n} \quad \tilde{\ }$ ) in addition to the bias 1);

So the filtering equation need to be modified as[6]:

$$\tilde{x} \quad \Big( \sum_{i,j} \quad R_{ij} \Big)^{-1} \Big( \sum_{i,j} R_{ij}^T (\hat{D}\hat{\alpha}_{ij} + < \tilde{\ } \quad \Big) \tag{10}$$

Where $R_{ij}$ is operator to extract a sub-block of image in position $(i, j)$ , the effect of $\left( \sum_{i,j} R_{ij}^T R_{ij} \right)^{-1} \sum_{i,j} R_{ij}^T$ is to average contributions from overlapping patches for a given pixel position, $< \tilde{\ }$ is the local mean.

K-SVD [12-13] method is used to get dictionary D, while the sparse coefficient matrix $\alpha$ is obtained by OMP algorithm.

## 3. NEW APPROACH

In the new approach of this paper, five steps are needed to implement speckle filtering, which are pixel structure classification, logarithmic transformation, sparse decomposition, reconstruction and final enhancement. Detail steps are described as follows:

Step A. Structure classification. According to the polarimetric characteristics of PolSAR image, all pixels in the image are divided into one of three classes, which are bright point or line targets, dark point or line targets, and other targets [7] to form a classification map,

Step B. Logarithmic transformation. This is performed on original power image to change multiplicative noise into additive.

Step C. Sparse decomposition. OMP algorithm and K-SVD algorithm are used to update dictionary D and coefficient $\alpha$ . Then the following steps are repeated $J$ times.

1) Sparse representation: Assuming D is fixed, the best sparse coefficients $\hat{\alpha}_{i,j}$ of each sub-block image are calculated with OMP algorithm.

2) Dictionary updating: Assuming $\hat{\alpha}_{i,j}$ is fixed, each column of the dictionary is updated by the K-SVD algorithm in turn.

The image noise variance is used as iteration termination conditions during calculating the best $\hat{\alpha}_{i,j}$ .When multi-look number is an integer, the noise variance of PolSAR image is [6]:

$$\mathrm{var} \quad \frac{\pi^2}{\ } - \sum_{m=1}^{M-1} \frac{1}{m^2} \tag{11}$$

M is the multi-look number of SAR image.

Step D. Image reconstruction. Image is constructed by formula (10) to get the noiseless image.

Step E. Image enhancement. According to the classification map, pixels in the reconstructed image are replaced with their original power value if they are classified as point and line targets in step A.

The processing flow chart is shown in Fig.1.

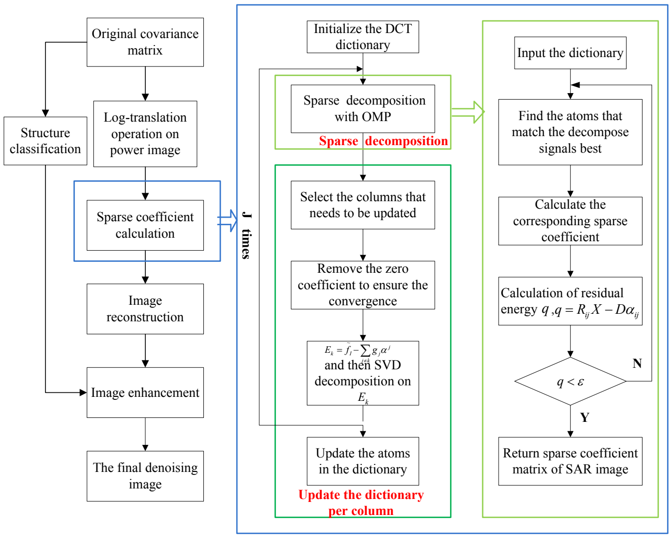


**Fig.1**. Flow Charts

## 4. EXPERIMENTAL RESULTS

Sixteen-look AIRSAR L-band PolSAR data of Half moon bay is used in the experiment. It contains abundant targets in the scene, such as ocean, farmland, buildings, grassland, airport, airplanes and a trihedral angle reflector. Image size is $300\times300$ . It's Pauli decomposition map are shown in Fig.2 and power image is shown in Fig.3.

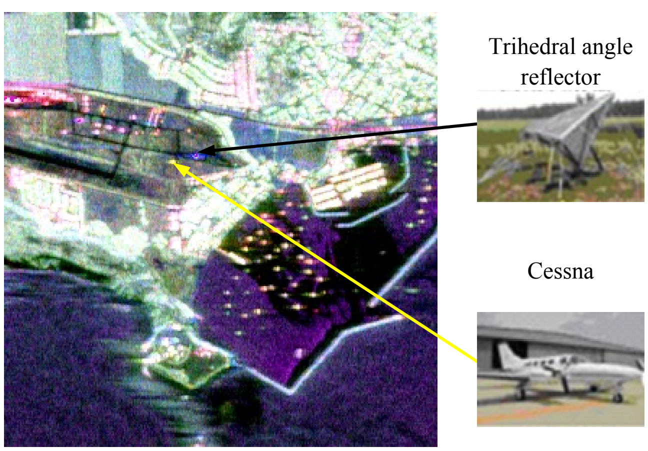


**Fig.2**. Pauli decomposition map of Half moon bay area.

Experimental parameters are set as follows: residual error $\varepsilon = C\sigma^2$ , the noise gains $C = 1.15$ , the noise variance $\sigma^2$ is calculated by the formula (11); the number of iterations $J = 5$ , the size of sub-blocks is $8\times8$ .

Classification map is shown in Fig.4. Black spots indicate the bright point or line targets . Gray spots represent dark point or line targets. White area represents other types of targets.

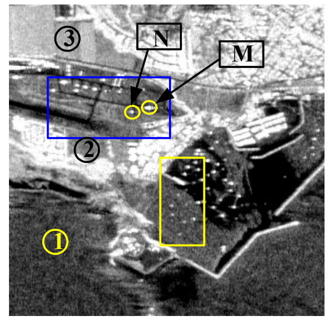


**Fig.3.** Original power image

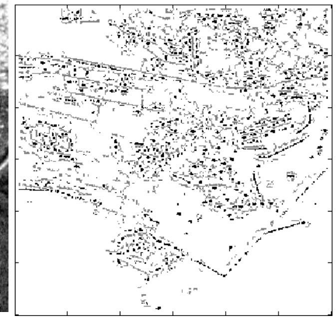

**Fig.4.** Structure classification map

Filtered images are shown in Fig.5.To demonstrate the validity of the proposed algorithm, we also show the experimental results of literature [6] in Fig.5.

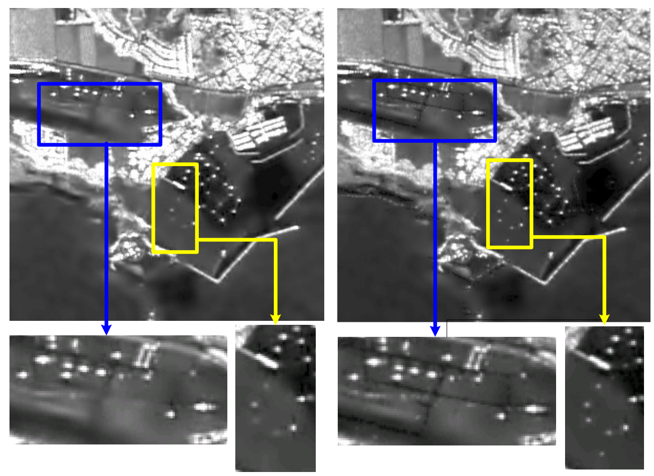

(a) Literature [6] algorithm (b)New algorithm

**Fig.5**. Power image after filtering

From Fig.5, we can see that the new algorithm show a better filtering result than Literature [6] such as the area in the rectangle frame where the point target(ships) and dark line targets(airport runway) are much clearer.

### 4.1. Effect on Speckle Reduction and Texture Features Retaining

ENL (Equivalent Number of Looks) is often used to describe the effect of speckle reduction. Here we select three uniform areas to calculate their ENL, which are ①ocean , ② grassland, ③ farmland (see Fig.3). The results are shown in Table 1.

Table 1.ENL of the two algorithms

| Area | Channel | Original image | Literature [6] algorithm | New algorithm |
|---|---|---|---|---|
| Ocean ① | HH | 13.86 | 584.39 | 584.39 |
| | HV | 16.94 | 318.55 | 311.89 |
| | VV | 11.74 | 308.91 | 301.35 |
| Grassland ② | HH | 11.31 | 180.14 | 180.04 |
| | HV | 11.35 | 239.82 | 239.14 |
| | VV | 11.12 | 218.63 | 219.28 |
| Farmland ③ | HH | 4.64 | 19.27 | 19.27 |
| | HV | 5.67 | 16.64 | 16.42 |
| | VV | 4.12 | 28.25 | 27.98 |

Table 1 show that both algorithms can get a higher ENL value compared with the original image, which means they can suppress speckles much better.

### 4.2. Effect on Edge-preserving

Effect on Edge-preserving is described by EPI [14] whose value is in the range of $[0,1]$ . The closer to 1 the EPI is, the better the effect of target edge-preserving is.

Table 2 shows the EPI value of the new algorithm and Literature [6]. By comparison, we can see the new algorithm has more effective edge-preserving ability.

Table 2. EPI value

| Algorithm | HH | HV | VV |
|---|---|---|---|
| Literature [6] algorithm | 0.8661 | 0.7840 | 0.8199 |
| New algorithm | 0.9582 | 0.9413 | 0.9207 |

### 4.3. Polarimetric Properties Preservation

As we known, Polarimetric properties is an important statistical factor of PolSAR, it can be described by a polarimetric characteristics chart.

Fig.6 shows the co-polarimetric and cross-polarimetric properties of trihedral angle reflector and aircraft (signed with “M” and “N” in Fig.4) after filtering. From Fig.6, we can see the trihedral angle reflector and dihedral aircraft target represent their polarimetric properties very well. That means the proposed algorithm behaves better performance on the polarimetric properties preservation.

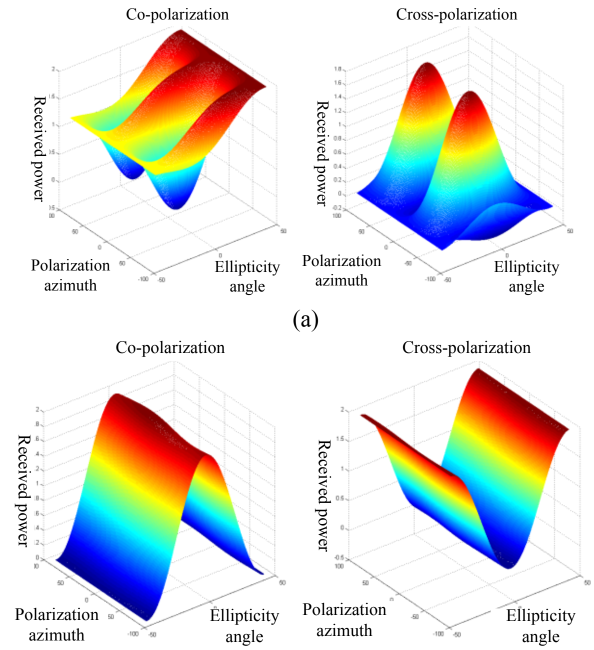


(b)

**Fig.6**. Polarimetric properties chart of targets after filtering. (a) Target M (b) Target N.

## 5. CONCLUSIONS

Combined with the sparse decomposition model and image structure features, this paper develops an effective algorithm for speckle reduction. The lower scattering characteristic and blurred point or line targets after sparse filtering are enhanced by initial classification map, which can make the targets edge much clearer and the weak scattering point stronger. Experimental results also illustrate that the proposed algorithm is more effective not only in speckle reduction but also in polarimetric properties preservation.

## ACKNOWLEDGEMENTS

This work is supported by the National Natural Science Foundation of China and Civil Aviation Administration of China (Item No. 61231017) and in part by the Fund of Civil Aviation University of China under grant ZXH2012D001 and 2012KYE03. The author would like to thank all teammates for the great effort.

## REFERENCES

[1] Elad M. and Aharon M.Image, “Denoising via Sparse and Redundant Representations Over Learned Dictionaries,” *[J]*, IEEE Transactions on Image Processing .15(12):3736-3745, 2006.

[2] Ye Chaomin, Qian Yuntao and Shen Yanhao, “Clustering based Sparse Model for Image Denoising,” *[J]*, *Signal Processing*, 27(10):1593-1598, 2011.

[3] Zhang X R and Wei Z L etc, “Sparse Representation based Spectral Clustering for SAR Image Segmentation,”*[C]*, Remote Sensing Image Processing, Geographic Information Systems, and Other Applications, Guilin, 2011:277-282.

[4] Jayaraman J and Thiagarajan, K N. etc, “Sparse Representations for Automatic Target Classification in SAR Images,” *[C]*. Proceedings of the 4th International Symposium on Communications, Control and Signal Processing, Limassol, Cyprus, 2010(8006):1-4.

[5] Zhang Haichao, Nasrabadi N M. and Huang T S, “Multi-View Automatic Target Recognition using Joint Sparse Representation, ”*[J]*. IEEE Transactions on Aerospace and Electronic Systems, 48(3):2481-2497, 2012.

[6] Samuel Foucher, “ SAR Image Filtering Via Learned Dictionaries and Sparse Representations,” *[C]*. IGARSS, Boston, 2008:229-232.

[7] Han Ping, Dong Fei and Wu Renbiao, “PolSAR Image Speckle Reduction Based on Multi-Stage Classification,” *[J].Systems Engineering and Electronics*, 34(7):1360-1365, 2012.

[8] Yin Zhongke, Xie Mei and Wang Jianying, “Image Denoising Based on Its Sparse Decomposition,” *[J]. Journal of University of Electronic Science and Technology of China*, 35(6):876-878, 2006.

[9] Zhao Yujuanl, Shui Penglang and Zhang Lingshuang, “Signal Sparse Approximation via Subspace Matching Pursuit,” *[J].Signal Processing*, 22(4):501-505, 2006.

[10] Pati Y C, Rezaiifar R and Krishnaprasad P S, “Orthogonal Matching Pursuit: Recursive Decomposition,”*[C]*. Proceedings of the 27th Annual Asilomar Conference on Signals, Systems and Computers, 1:40-44, 1993.

[11] Mairal J, Sapiro G and Elad M, “Learning Multiscale Sparse Representations for Image and Video Restoration,” *[J].SIAM Multiscale Modeling and Simulation*. 2008. 7(1):214-241.

[12] Aharon M，Elad M and Bruckstein A, “The K-SVD: An Algorithm for Designing Over-complete Dictionaries for Sparse Representation,” *[J]．IEEE Transactions on Signal Processing*,54(11):4311-4322, 2006.

[13] Elad M and Aharon M, “Image Denoising Via Learned Dictionaries and Sparse Representation,” *[C]*. Processing IEEE Computer Society Conference , 2006(1):895-900.

[14] Wang Chao etc, “Fully polarimetric synthetic aperture radar image processing,” *[M]* Beijing: Science Press, 2008: 68-69.